p50–NF-κB Complexes Partially Compensate for the Absence of RelB: Severely Increased Pathology in $p50^{-/-}relB^{-/-}$ Double-knockout Mice

By Falk Weih,* Stephen K. Durham,‡ Debra S. Barton,‡ William C. Sha,§ David Baltimore,§ and Rodrigo Bravo*

*From the *Department of Oncology, ‡Department of Experimental Pathology, Bristol-Myers Squibb Pharmaceutical Research Institute, Princeton, New Jersey 08543-4000; and the §Department of Biology, Massachusetts Institute of Technology, Cambridge, Massachusetts 02139*

Summary

RelB-deficient mice ($relB^{-/-}$) have a complex phenotype including multiorgan inflammation and hematopoietic abnormalities. To examine whether other NF-κB/Rel family members are required for the development of this phenotype or have a compensatory role, we have initiated a program to generate double-mutant mice that are deficient in more than one family member. Here we report the phenotypic changes in $relB^{-/-}$ mice that also lack the p50 subunit of NF-κB ($p50^{-/-}$). The inflammatory phenotype of $p50^{-/-}relB^{-/-}$ double-mutant mice was markedly increased in both severity and extent of organ involvement, leading to premature death within three to four weeks after birth. Double-knockout mice also had strongly increased myeloid hyperplasia and thymic atrophy. Moreover, B cell development was impaired and, in contrast to $relB^{-/-}$ single knockouts, B cells were absent from inflammatory infiltrates. Both $p50^{-/-}$ and heterozygous $relB^{-/+}$ animals are disease-free. In the absence of the p50, however, $relB^{-/+}$ mice ($p50^{-/-}relB^{-/+}$) had a mild inflammatory phenotype and moderate myeloid hyperplasia. Neither elevated mRNA levels of other family members, nor increased κB-binding activities of NF-κB/Rel complexes could be detected in single- or double-mutant mice compared to control animals. These results indicate that the lack of RelB is, in part, compensated by other p50-containing complexes and that the "classical" p50-RelA–NF-κB activity is not required for the development of the inflammatory phenotype.

Cellular decisions involved in growth, differentiation, and development require the coordinated expression of a wide variety of genes. The transcriptional regulation of genes is mediated by factors that bind singly or in association with other proteins to *cis*-regulatory sequences found in promoters, enhancers, and silencers. These transcription factors frequently form families in which individual members have distinct or similar functions.

The NF-κB/Rel family of transcription factors represents a group of homodimeric and heterodimeric complexes that plays an important role in the function of lymphocytes and other cells of hematopoietic origin. Five members of this family have been identified in vertebrates: NF-κB1 (encoding the precursor molecule p105 that is proteolytically processed to p50), NF-κB2 (encoding the precursor p100 and the processed form of p52), RelA (p65), RelB, and c-Rel (Rel). One hallmark of the family is a highly conserved domain of ~300 amino acids, termed the Rel homology domain, that contains sequences important for dimerization, DNA binding, and nuclear localization. In most cell types NF-κB/Rel proteins associate with the inhibitor molecule IκB forming an inactive cytoplasmic complex that can be activated by a wide range of stimuli leading to degradation of IκB and nuclear translocation of the NF-κB/Rel proteins and their binding to so-called κB sequence motifs. Many target genes are involved in immune, inflammatory, acute phase, and stress responses (1–7).

Recent evidence using mice with targeted disruptions for individual members of the NF-κB/Rel family indicates that the different proteins play distinct biological roles. For example, p50-deficient mice appear normal and lymphocyte development is not impaired. However, these animals have multifocal defects in immune responses and B cells are defective in mitogenic activation and specific antibody production (8, 9). Mice with a targeted disruption of RelA are embryonic lethal due to a defect in liver development (10). Mature B and T cells from mice that lack c-Rel were found to be unresponsive to most mitogenic stimuli (11, 12).

RelB, originally identified as an immediate-early gene in growth factor-induced fibroblasts (13, 14), is expressed predominantly in lymphoid tissues where RelB heterodimers represent the major constitutive κB-binding activity (15–18). In thymus, *relB* transcripts are confined to the medulla and high levels of RelB are expressed in the nucleus of inter-

 J. Exp. Med. © The Rockefeller University Press • 0022-1007/97/04/1359/12 $2.00
Volume 185, Number 7, April 7, 1997 1359–1370

digitating dendritic cells (DC)[1]. In addition, lower levels of RelB expression can be detected in macrophages as well as B and T cells (15, 16, 18–20).

Mice with a targeted disruption of RelB have pathological changes including inflammatory cell infiltration in several organs, myeloid hyperplasia, and splenomegaly due to extramedullary hematopoiesis. RelB is also required for the normal development of thymic medulla and antigen-presenting DC. Besides the pathological changes, RelB-deficient mice have multifocal defects in cellular and humoral immune responses (21 and 21a). Similarly, a mutation disrupting the *relB* locus by the random integration of transgene sequences resulted in mice with a syndrome of excess production of macrophages and granulocytes, reduced populations of thymic dendritic and medullary epithelial cells, and impaired antigen-presenting cell function (22).

Different NF-κB/Rel complexes have different sequence preferences and transcriptional activation properties. However, the DNA binding domain is highly conserved between NF-κB/Rel family members and p50-RelA, p50-RelB, or p50-c-Rel heterodimers can bind to similar regulatory κB sequences and activate transcription of target genes (23–25). Although the phenotypic changes in $relB^{-/-}$ mice show that RelB function is crucial for a normal hematopoietic system (21, 22), it is possible that other members of the NF-κB/Rel family may, at least in part, functionally compensate for the lack of RelB. p50-deficient mice do not have any pathological changes and the absence of the "classical" p50-RelA–NF-κB activity as well as other p50-containing NF-κB/Rel complexes (8) make this mutant mouse line a useful model system to address functional redundancy within the NF-κB/Rel family. In addition, $p50^{-/-}relB^{-/-}$ double-knockout mice may provide an answer to the question of whether p50-RelA–NF-κB complexes are required in the effector cells that mediate the $relB^{-/-}$ phenotype.

In this report we compare the phenotype of $p50^{-/-}$ and $relB^{-/-}$ single-mutant, $p50^{-/-}relB^{-/-}$ double-mutant, and $p50^{-/-}relB^{-/+}$ mice, and focus on the different cell types involved in the pathological changes observed in these animals. The results indicate that the lack of RelB is partially compensated by other p50-containing complexes and that the p50-RelA–NF-κB activity is not essential for the development of the inflammatory phenotype in RelB-deficient mice.

Materials and Methods

Mice. RelB- and p50-deficient mice were originally established from $relB^{-/+}$ (129/Sv × C57BL/6J background) and $p50^{-/+}$ (129/Ola × C57BL/6J background) mice, respectively, and were subsequently maintained by intercrosses (8, 21). Tail DNA was prepared as described (26). The genotype of RelB-deficient mice was determined by PCR amplification (1 min at 95°C, 1.5 min at 60°C, and 1 min at 72°C for 33 cycles) using primer pairs recognizing the intact *relB* gene (5′-GTG GTG CCC GGG AAT AGG ATT GCT G-3′ and 5′-CCA TTT TGC TCT GGG TCT GTG TCT G-3′) and the targeted *relB-neo* locus (5′-CAT CGA CGA ATA CAT TAA GGA GAA CGG-3′ and 5′-AAA TGT GTC AGT TTC ATA GCC TGA AGA ACG-3′). PCR amplification conditions for p50-deficient mice were 1 min at 95°C and 2 min at 66°C for 30 cycles using primers specific for the intact *nfkb1* gene (5′-GCA AAC CTG GGA ATA CTT CAT GTG ACT AAG-3′ and 5′-ATA GGC AAG GTC AGA ATG CA CAG AAG TCC-3′) and the targeted *nfkb1-neo* locus (5′-AAA TGT GTC AGT TTC ATA GCC TGA AGA ACG-3′). All animals were housed and bred within the same room (in Veterinary Sciences Department of Bristol-Myers Squibb Pharmaceutical Research Institute, Princeton, NJ). The absence of pathogens was assessed by extensive, periodic, comprehensive serology, and histopathology of sentinel animals housed within the same room.

Histopathology and Immunohistochemistry. Histopathological analyses were performed on a minimum of three animals per age group and genotype. Tissues were immersion-fixed in 10% buffered formalin, embedded in paraffin blocks, and processed by routine methods. Sections (4–6 μm thick) were stained with hematoxylin and eosin, and examined by light microscopy. For immunohistochemical staining of $CD4^+$ and $CD8^+$ T cells, tissues were frozen in O.C.T.-embedding medium (Miles Inc., Elkhart, IN), sectioned at 8 μm, and immediately fixed in buffered formalin/acetone. Sections were blocked with avidin D/biotin reagents (Vector Labs., Inc., Burlingame, CA), followed by 0.5% casein in PBS, and incubated with purified CD4- or CD8-specific mAb from PharMingen (San Diego, CA; clone RM4-5 diluted 1:50 and clone 53-6.7 diluted 1:20, respectively) for 180 min at room temperature. For immunohistochemical staining of B cells, mature macrophages, and neutrophils, formalin-fixed paraffin sections were treated with 0.1% trypsin at 37°C for 20 min, blocked with avidin D/biotin reagents and normal mixed serum (Shandon Inc., Pittsburgh, PA), and incubated with purified specific mAbs (clone RA3-6B2 diluted 1:300 [PharMingen] and clone F4/80 diluted 1:10 and clone 7/4 diluted 1:50 [both from Harlan Bioproducts for Science Inc., Indianapolis, IN]) for 90 min a room temperature. Endogenous peroxidase activity was quenched in 3% hydrogen peroxide in PBS for 10 min at room temperature. Incubation with a biotinylated secondary Ab (mouse-absorbed anti–rat IgG from rabbit, diluted 1:100) was for 30 min, followed by avidin-linked peroxidase for 30 min, followed by diaminobenzidine chromogen for 3 min, and hematoxylin counterstain for 1 min. Unless otherwise stated, all reagents were obtained from Vector Labs., Inc. For negative control slides, the primary Ab was substituted with normal mixed serum.

Flow Cytometry. Flow cytometry was done using a flow cytometer and cell sorter (Coulter Epics Profile II; Coulter Corp., Hialeah, FL). Splenocytes and bone marrow cells were isolated and mature red blood cells were lysed according to standard procedures (27). Cell suspensions were incubated with mAbs (≤1 μg each/10^6 cells) for 30 min on ice, spun, and washed with PBS/2% fetal calf serum. Conjugated CD4-FITC, CD8-PE, and CD45R/B220-FITC mAbs were obtained from GIBCO BRL (Gaithersburg, MD); TCR-α/β-FITC, IgM-FITC, and Gr-1-FITC mAb were from PharMingen; Mac-1-PE mAb was from Boehringer Mannheim (Indianapolis, IN). An average of 10^4 cells was recorded in each case.

Semi-Quantitative Reverse Transcription–PCR Analyses. Total thymus RNA from 2-wk-old mice was isolated using TRIzol according to the manufacturer's instructions (GIBCO BRL). cDNA was synthesized from 2 μg total RNA (Superscript Preamplifica-

[1]*Abbreviations used in this paper:* DC, dendritic cells; DOC, deoxycholate; DP, double positive; EMSA, electrophoretic mobility shift assays.

tion System; GIBCO BRL). Semi-quantitative PCR was performed under conditions where amplification of the cDNAs was linearly dependent on the concentration of the corresponding mRNAs (28, 29). The sequences of the primers were: for *nfkb1*, 5′-GCA CCG TAA CAG CAG GAC CCA AGG ACA-3′ and 5′-CCC GTC ACA CAT CCT GCT GTT CTG TCC ATT CT-3′; for *nfkb2*, 5′-GCC TGG ATG GCA TCC CCG-3′ and 5′-CTT CTC ACT GGA GGC ACC T-3′; for *relA*, 5′-TAG CCT TAC TAT CAA GTG TCT TCC TCC-3′ and 5′-GTT CAG AGC TAG AAA GAG CAA GAG TCC-3′; for *relB*, 5′-CCT CTC TTC CCT GTC ACT AAC GGT CTC-3′ and 5′-ACG CTG CTT TGG CTG CTC TGT GAT G-3′; for c-*rel*, 5′-TGG CTG ACT GAC TCA CTG ACT GAC TGA CTC GTG CCT TGC-3′ and 5′-CCA ACT AAA TCA TGA GGA TGA GGC TTA TAT GGA TCA TTC-3′; for *ikba*, 5′-CAG GAC TGG GCC ATG GAG GG-3′ and 5′-TGG CCG TTG TAG TTG GTG GC-3′; for *ikbb*, 5′-CCC TTC CTG GAT TTC CTC CTG GGC TTT TC-3′ and 5′-GTG GGG TCA GCA CCG GCT TTC AGG AGA-3′; and for *β-actin*, 5′-AGA GGT ATC CTG ACC CTG AAG TAC C-3′ and 5′-CCA CCA GAC AAC ACT GTG TTG GCA T-3′.

Electrophoretic Mobility Shift Assays. Whole cell extracts from 2-wk-old thymuses were prepared as described (16). The oligodeoxynucleotide comprising a palindromic, κB-binding site has been described previously (13, 24). 4 μg of thymus extract were incubated with 10 fmol of the radiolabeled probe in 10 mM Tris × HCl, pH 7.5, 50 mM NaCl, 1 mM EDTA, 5 mM dithiothreitol, 5% glycerol, and 0.6 μg herring sperm DNA; κB-binding activity was analyzed in electrophoretic mobility shift assays (EMSAs) as previously described (18). Extracts were activated by treatment with 0.6% deoxycholate (DOC) for 15 min on ice followed by the addition of NP-40 to a final concentration of 1.2%. As a control, binding of unactivated extracts was also performed in the presence of 1.2% NP-40. Integrity of extracts was checked with an octamer binding site.

Results

Increased Mortality of $p50^{-/-}relB^{-/-}$ Double-knockout Mice. Mice with a targeted deletion of p50 are fertile, whereas the majority of RelB-deficient mice are sterile due to marked inflammatory infiltrates in the reproductive organs of males and females older than 40 d (8, 21). Therefore, the $p50^{-/-}$ mutation was crossed into a $relB^{-/+}$ background generating $p50^{-/-}relB^{-/+}$ animals that were interbred to obtain $p50^{-/-}relB^{-/-}$ double-mutant mice. The resulting litters were normal in size, all animals appeared healthy at the time of birth, and $p50^{-/-}relB^{+/+}$, $p50^{-/-}relB^{-/+}$, and $p50^{-/-}relB^{-/-}$ mice were born at expected Mendelian ratios, demonstrating that $p50^{-/-}relB^{-/-}$ double-knockout mice can develop to birth (data not shown).

2–3 wk after birth, however, all the $p50^{-/-}relB^{-/-}$ animals were runted, lethargic, had abdominal distension, and their body weights were reduced 30–50%, compared to control littermates; $relB^{-/-}$ mice of the same age were less severely affected (Fig. 1 *A*). The disease progressed rapidly in $p50^{-/-}relB^{-/-}$ mice leading to premature death of >95% of the animals between 2 and 4 wk of age (Fig. 1 *B*). $relB^{-/-}$ single-knockout mice also had increased mortality, but only 33% died within the first 4 wk after birth. Heterozygous $relB^{-/+}$ on a wild-type or $p50^{-/-}$ background did not have increase mortality, although several $p50^{-/-}relB^{-/+}$ mice of 5 mo and older appeared sick and died prematurely (Fig. 1 *B* and data not shown). At necropsy of 20-d-old mice, marked thymic atrophy, splenomegaly, and liver and kidney turgidity were observed in all $p50^{-/-}relB^{-/-}$ double knockouts. Moderate thymic atrophy and splenomegaly was observed in $relB^{-/-}$ single-knockout animals. Wild-type controls, $p50^{-/-}$ single knockouts, and $relB^{-/+}$ mice were nonremarkable (Fig. 1 *C* and data not shown).

Multiorgan Inflammation: Increased Severity and Extent in $p50^{-/-}relB^{-/-}$ Double-knockout Mice. The histopathological findings in 20-d-old mice of various genotypes are summarized in Table 1. No changes were observed following an extensive histopathological examination of lymphoid and nonlymphoid tissues from several wild-type, $relB^{-/+}$, and $p50^{-/-}$ animals. A minimal inflammatory phenotype accompanied by a moderate myeloid hyperplasia occurred in heterozygous $relB^{-/+}$ mice in the absence of p50 ($p50^{-/-}relB^{-/+}$). $relB^{-/-}$ single-knockout mice had a moderate multiorgan infiltrate.

In contrast, $p50^{-/-}relB^{-/-}$ double-knockout mice by day 20 developed an inflammatory infiltrate that was of

Table 1. *Histopathology Summary of 3–4 wk-old Mice of Different Genotypes*

	$p50^{-/-}$	$p50^{-/-}relB^{-/+}$	$relB^{-/-}$	$p50^{-/-}relB^{-/-}$
Thymus	NR	NR	G2-3 atrophy	G4 atrophy
Spleen	NR	G1 EMH	G2-3 EMH	G4 EMH
Bone marrow	NR	G1 MH	G2-3 MH	G4 MH
Lung	NR	G1 PV LC	G3 PV MXE	G4 PV MXE
Liver	NR	G1 PP MX	G3 PP MXE	G4 PP MXE
Kidney	NR	NR	NR	G3 PV MNE
Heart	NR	NR	NR	G2 MN

NR, nonremarkable (as compared to similarly aged wild-type and $relB^{-/+}$ mice) *G1*, minimal; *G2*, mild; *G3*, moderate; *G4*, marked; *EMH*, extramedullary hematopoiesis; *MH*, myeloid hyperplasia; *PV*, perivascular; *PP*, periportal; *LC*, lymphocytes; *MX*, mixed (both polymorphonuclear and mononuclear cells); *E*, extending into the surrounding parenchyma from a perivascular or periportal orientation; *MN*, mononuclear cells.

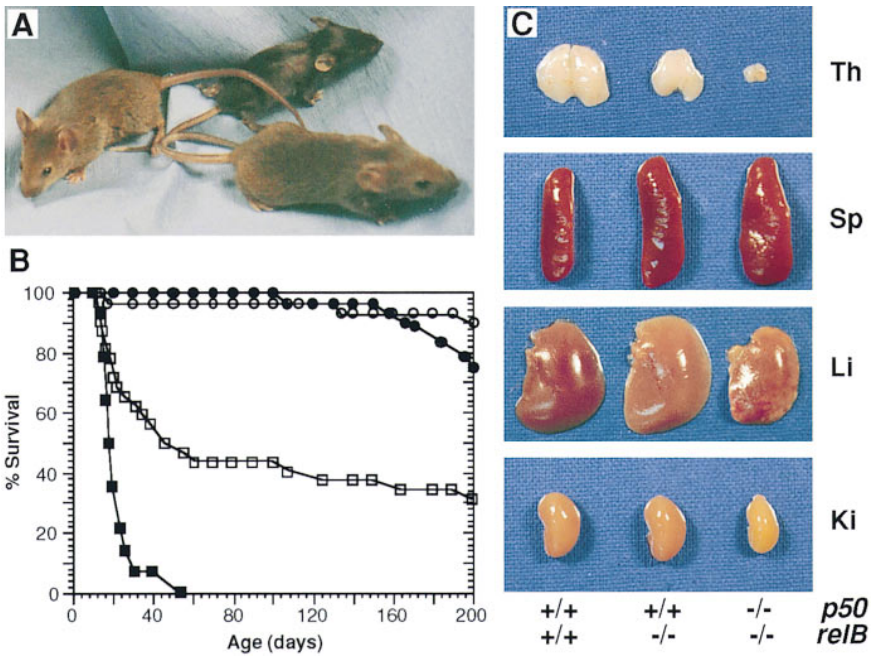

Figure 1. (*A*) Gross appearance of 20-d-old wild-type (*right*), $relB^{-/-}$ (*left*), and $p50^{-/-}relB^{-/-}$ (*middle*) mice. (*B*) Survival of $relB^{-/+}$, $p50^{-/-}relB^{-/+}$, $relB^{-/-}$, and $p50^{-/-}relB^{-/-}$ mice. Surviving mice expressed as a percentage of the initial number of animals in each genotype group are plotted. $relB^{-/+}$ mice (○); $p50^{-/-}relB^{-/+}$ mice (●); $relB^{-/-}$ mice (□); and $p50^{-/-}relB^{-/-}$ mice (■). (*C*) Thymus (*Th*), spleen (*Sp*), liver (*Li*), and kidney (*Ki*) from 20-d-old wild-type, $relB^{-/-}$, and $p50^{-/-}relB^{-/-}$ animals. Genotypes are indicated at the bottom.

greater severity and extent of organ system involvement as compared to $relB^{-/-}$ single-knockout animals. Interestingly, 8–10-d-old $p50^{-/-}relB^{-/-}$ mice were only slightly more affected than similarly aged $relB^{-/-}$ animals. Thereafter, the infiltrate in RelB-deficient mice progressed much more rapidly and aggressively in the absence of the p50 subunit of NF-κB, and was reflected by increased mortality (Fig. 1 *B* and data not shown). Similar to $relB^{-/-}$ single-knockout animals, the lung and liver were also markedly affected in $p50^{-/-}relB^{-/-}$ double-knockout mice. In the lung of

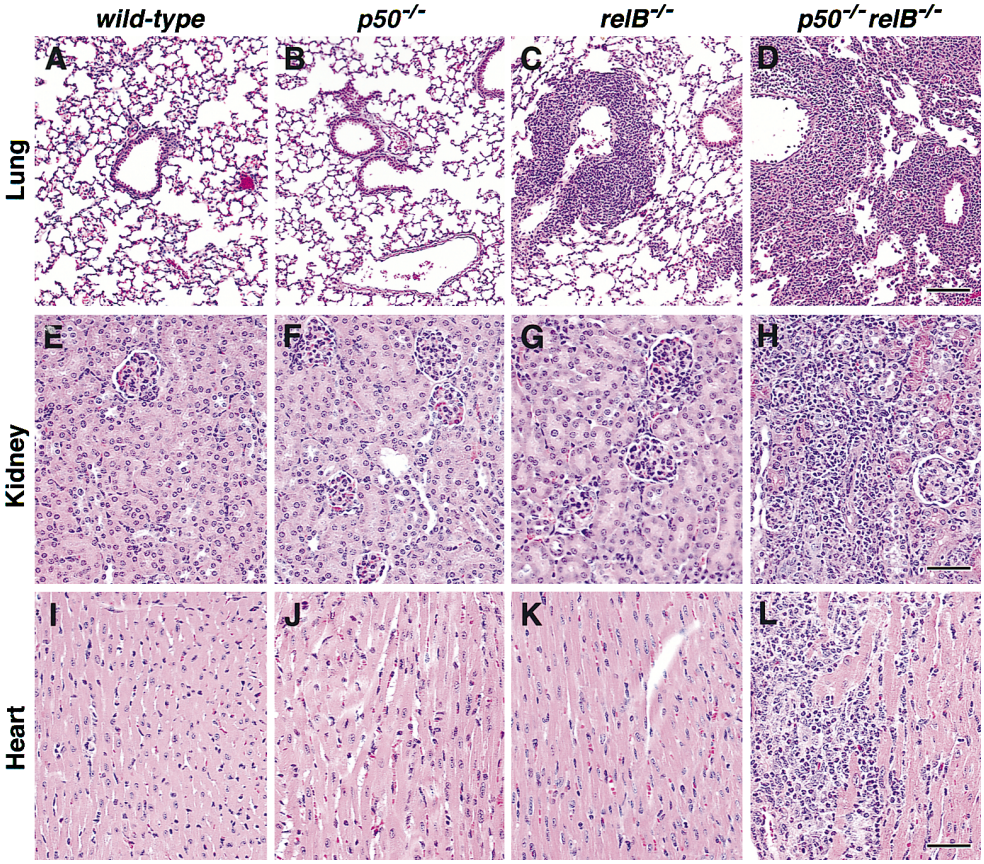

Figure 2. Histopathological analysis of wild-type, $p50^{-/-}$, $relB^{-/-}$, and $p50^{-/-}relB^{-/-}$ mice. Lung (*A–D*), kidney (*E–H*), and heart (*I–L*) sections from 20-d-old mice stained with hematoxylin and eosin. (*A*, *E*, and *I*) Wild-type control; (*B*, *F*, and *J*) $p50^{-/-}$ single mutant; (*C*, *G*, and *K*) $relB^{-/-}$ single mutant; (*D*, *H*, and *L*) $p50^{-/-}relB^{-/-}$ double mutant. Bars: (*A–D*), 100 μm; (*E–L*), 50 μm.

double-knockouts, the infiltrate was in a perivascular and periairway orientation that extended into and effaced the surrounding parenchyma, whereas in the *relB*$^{-/-}$ single knockouts, the infiltrate was predominantly restricted to a perivascular orientation (Fig. 2 *A–D*). In the liver of *relB*$^{-/-}$ and *p50*$^{-/-}$*relB*$^{-/-}$ mice, the infiltrate originated in periportal areas and extended into surrounding hepatocellular trabeculae and sinusoids. However, the infiltrate in double-knockout animals was so severe that infarction was commonplace, most likely resulting from infiltrate-induced interference with vascular flow (data not shown). In addition, the inflammatory infiltrate of 20-d-old double-knockout mice also involved kidney (Fig. 2, *E–H*), heart (Fig. 2, *I–L*), striated musculature, and salivary glands, organs that were not affected in 3-wk-old *relB*$^{-/-}$ single-knockout mice. Myeloid hyperplasia in the bone marrow and spleen was also more pronounced in double knockouts as compared to *relB*$^{-/-}$ single-knockout animals (data not shown).

Role of T Cells, B Cells, Macrophages, and Neutrophils in the Inflammatory Phenotype. To examine the cellular composition of the inflammatory infiltrates in nonlymphoid tissues in more detail, lung and liver sections from 20-d-old wild-type controls, *relB*$^{-/-}$, and *p50*$^{-/-}$*relB*$^{-/-}$ mice were analyzed by immunohistochemical criteria. Only resident leukocyte populations were detected in control tissues stained with the different mAbs (Fig. 3, *A* and *D*; and Fig. 4, *A*, *D*, and *G*). In contrast, abundant staining was observed in pulmonary infiltrates of both *relB*$^{-/-}$ and *p50*$^{-/-}$*relB*$^{-/-}$ mice with mAbs specific for CD4$^+$ helper T cells (Fig. 3, *B* and *C*) and CD8$^+$ cytotoxic T cells, although a smaller number of CD8$^+$ lymphocytes occurred both quantitatively and proportionally in the infiltrates of double-knockout mice (Fig. 3 *E* and *F*). Prominent infiltrates, consisting predominantly of CD4$^+$ and CD8$^+$ lymphocytes, were observed in the lung and liver of these animals as early as 10 d after birth, suggesting that T cells are crucially involved in the onset of the inflammatory phenotype (data not shown).

To examine which non–T cell types are involved in the inflammatory infiltrates, liver sections from 20-d-old wild-type, *relB*$^{-/-}$, and *p50*$^{-/-}$*relB*$^{-/-}$ mice were stained with mAbs specific for B cells, macrophages, and neutrophils (Fig. 4). B cells were readily detected within the periportal infiltrate in sections from *relB*$^{-/-}$ mice (Fig. 4 *B*). In marked contrast, the inflammatory infiltrate in *p50*$^{-/-}$*relB*$^{-/-}$ liver contained very few B cells (Fig. 4 *C*), indicating that B cells are not required for the development of the inflammatory phenotype in *p50*$^{-/-}$*relB*$^{-/-}$ animals. Kupffer cells, specialized tissue macrophages residing along hepatic sinusoids, showed strong positive staining in wild-type mice as compared to *relB*$^{-/-}$ and *p50*$^{-/-}$*relB*$^{-/-}$ animals (Fig. 4, *D–F*). Little F4/80-positive staining was detected within the infiltrates of single- and double-knockout mice (Fig. 4, *E* and *F*). This finding, coupled with the observation that few infiltrative cells had morphological criteria of macrophages, suggest that this cell population is not a prominent component of the inflammatory phenotype of these animals at this age. Since adult RelB-deficient mice have increased granulopoiesis in bone marrow and spleen (21, 22), we examined whether polymorphonuclear leukocytes are an important component of the inflammatory infiltrates. Markedly increased numbers of neutrophils were detected in the periportal infiltrates of *p50*$^{-/-}$*relB*$^{-/-}$ mice compared to *relB*$^{-/-}$ animals (Fig. 4, *G–I*). Similar results were obtained when lung sections were stained for B cells, macrophages, and neutrophils (data not shown).

Increased Myeloid Hyperplasia and Impaired B Cell Development in p50$^{-/-}$*relB*$^{-/-}$ *Mice.* Flow cytometric analysis of 3-wk-old *p50*$^{-/-}$*relB*$^{-/-}$ double-knockout mice revealed marked alterations in thymus, spleen, and bone marrow cell subpopulations. Mice deficient in the p50 subunit of NF-κB, like heterozygous *relB*$^{-/+}$ mice, do not have any changes compared to wild-type animals (8, 21; data not shown) and were used as controls. We also included *relB*$^{-/+}$ mice on a *p50*$^{-/-}$ background (*p50*$^{-/-}$*relB*$^{-/+}$) since these animals develop a mild inflammatory phenotype (see Table 1). CD4$^+$CD8$^+$ double positive (DP) TCR^{lo} thymocytes were dramatically reduced in double knockouts, whereas CD8$^+$ and, in particular, CD4$^+$ single positive TCR^{hi} T cells were relatively increased (Fig. 5 *A*). Mature T cells were present in *p50*$^{-/-}$*relB*$^{-/-}$ spleen whereas B220$^+$IgM$^+$ B cells were markedly reduced. In contrast, numbers of myeloid cells (Mac-1$^+$, Gr-1$^+$, 7/4$^+$) were dramatically increased (Fig. 5 *B* and data not shown). With respect to the reduced number of B cells, *p50*$^{-/-}$*relB*$^{-/-}$ double-knockout spleens were characterized by poorly-developed B cell follicles, hyperplastic periarterial lymphatic sheath (T cell) areas, and indiscrete marginal zones (data not shown). Flow cytometric analysis of bone marrow cells also revealed increased numbers of myeloid cells and markedly reduced B220$^+$ IgM$^-$ and B220$^+$IgM$^+$ B cell populations (Fig. 5 *C*). Interestingly, *p50*$^{-/-}$*relB*$^{-/+}$ mice also had a moderate reduction in splenic B cells and increased numbers of myeloid cells in the bone marrow, but normal T cell subsets in thymus and spleen (Fig. 5, *A–C*).

Since the interpretation of the results obtained from 3–4-wk old animals is hampered by the severe pathological changes in lymphoid organs of *p50*$^{-/-}$*relB*$^{-/-}$ double-knockout mice, we analyzed 2-wk-old animals by flow cytometry. At this age, both *relB*$^{-/-}$ and *p50*$^{-/-}$*relB*$^{-/-}$ mice show a milder phenotype, and the pathological differences between these two mutant lines are less pronounced. Wild-type animals were included as a control; similar results were obtained with *p50*$^{-/-}$ or *relB*$^{-/+}$ mice (data not shown). Similar to the results shown in Fig. 5, although less severe, 2-wk-old *p50*$^{-/-}$*relB*$^{-/-}$ mice had decreased numbers of DP thymocytes and an increased population of thymic CD4$^+$TCR^{hi} T cells (Fig. 6 *A*). T cell subsets in double-knockout spleen were normal, but both B220$^+$IgM$^-$ and B220$^+$IgM$^+$ B cell populations were reduced, and the number of myeloid cells was increased (Fig. 6 *B*). Similarly, the number of Gr-1$^+$ cells was increased in double-knockout bone marrow while both B cell subpopulations were markedly reduced (Fig. 6 *C*). In contrast, *relB*$^{-/-}$ mice of the same age had only moderate myeloid hyperplasia in spleen and a very mild reduction in B220$^+$IgM$^+$ B cells compared to wild-type littermates (Fig. 6 and data not shown).

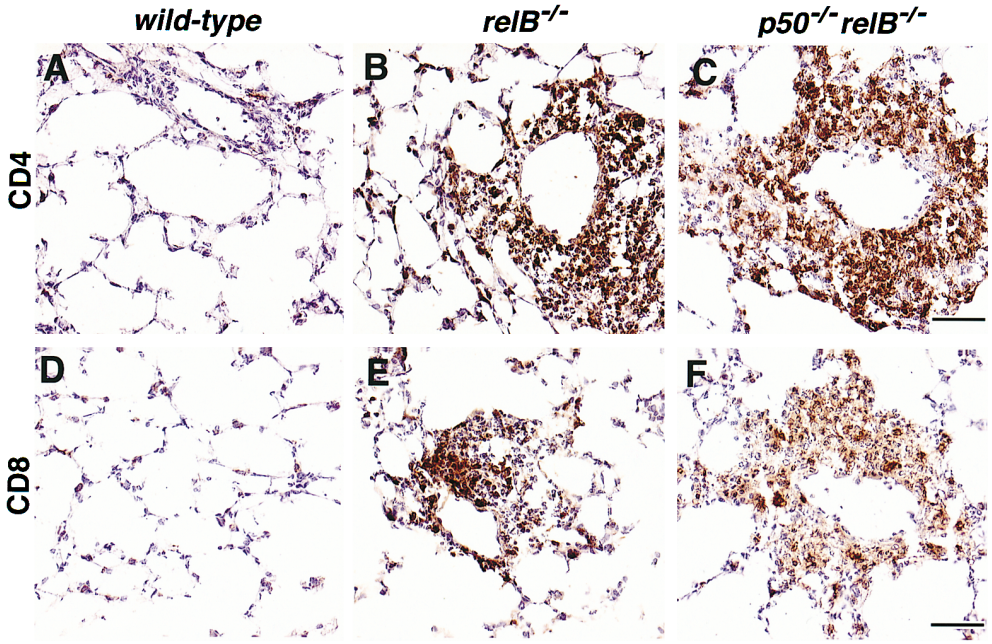

Figure 3. Immunohistochemical detection of T cells in lungs from 20-d-old wild-type, *relB*$^{-/-}$, and *p50*$^{-/-}$*relB*$^{-/-}$ mice. (*A–C*) Lung sections stained with an mAb specific for CD4^{+} T helper cells. (*D–F*) Lung sections stained with an mAb specific for CD8^{+} cytotoxic T cells. (*A* and *D*) Wild-type control; (*B* and *E*) *relB*$^{-/-}$ single mutant; (*C* and *F*) *p50*$^{-/-}$*relB*$^{-/-}$ double mutant. Bars, 50 μm.

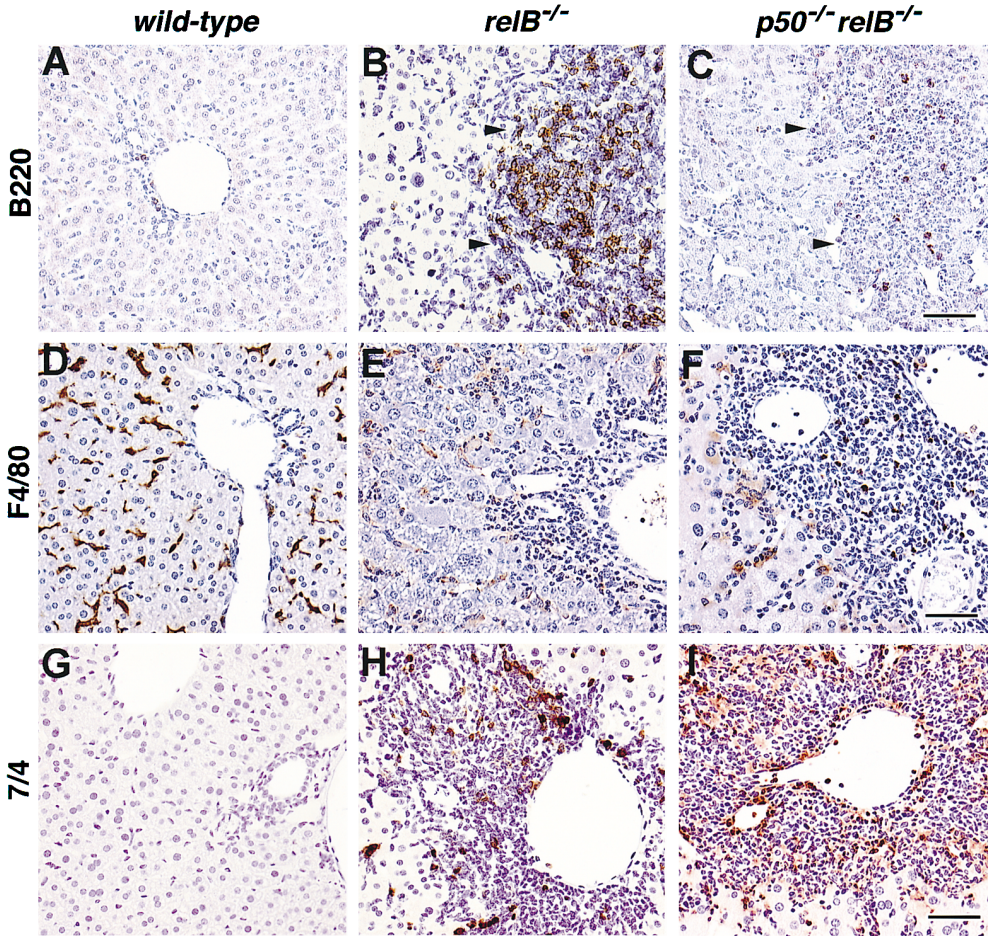

Figure 4. Immunohistochemical detection of B cells, macrophages, and neutrophils in liver from 20-d-old wild-type, *relB*$^{-/-}$, and *p50*$^{-/-}$*relB*$^{-/-}$ mice. (*A–C*) Liver sections stained with a B cell–specific mAb (B220). (*D–F*) Liver sections stained with an mAb specific for macrophages (F4/80). (*G–I*) Liver sections stained with an mAb specific for neutrophils (7/4). (*A*, *D*, and *G*) Wild-type control; (*B*, *E*, and *H*) *relB*$^{-/-}$ single mutant; (*C*, *F*, and *I*) *p50*$^{-/-}$ *relB*$^{-/-}$ double mutant. Arrows in *B* and *C* mark the periportal inflammatory infiltrate. Bars, 50 μm.

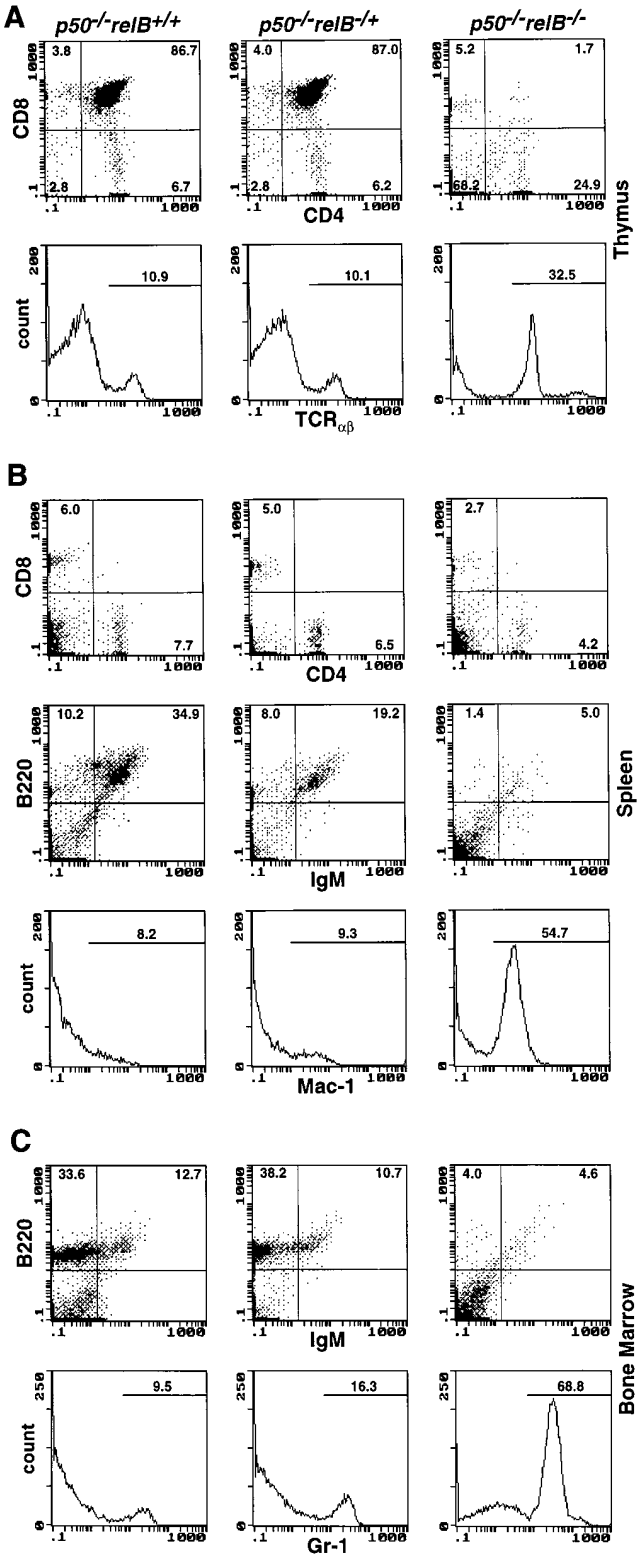

Figure 5. Flow cytometric analysis of 3-wk-old $p50^{-/-}$, $p50^{-/-}relB^{-/+}$, and $p50^{-/-}relB^{-/-}$ mice. Thymus (*A*), spleen (*B*), and bone marrow (*C*) single cell suspensions were analyzed for surface expression of CD4, CD8, and TCR-α/β (T cells), B220 and IgM (B cells), Mac-1 (macrophages and granulocytes), and Gr-1 (granulocytes). Genotypes are depicted above representative plots. Numbers indicate subpopulation percentages.

Expression and DNA Binding of NF-κB/Rel Family Members in Single- and Double-mutant Mice. To examine whether there is any compensatory upregulation of other family members in mice lacking p50, RelB, or both, mRNA levels of all NF-κB/Rel family members and IκBα/β in thymus were determined by semi-quantitative reverse transcription–PCR. Expression of β-actin was used as a reference (Fig. 7). Whereas *nfkb1* and *relB* transcripts were absent in the respective mutant lines, mRNAs specific for *relA*, c-*rel*, *ikba*, and *ikbb* were readily detected in all genotypes examined. Expression of these genes was not significantly altered but *nfkb2* mRNA levels were reduced in both single- and double-mutant mice, suggesting that *nfkb2* expression may be regulated by p50–RelB heterodimers. Interestingly, p52 protein levels were only slightly reduced in extracts from single- or double-knockout mice (8, 21; data not shown). These results indicate that there is no compensatory upregulation of other NF-κB/Rel family members in the absence of p50, RelB, or both.

To correlate mRNA levels with κB-binding activity, EMSA with thymus extracts from wild-type, $p50^{-/-}$, $relB^{-/-}$, and $p50^{-/-}relB^{-/-}$ mice were performed (Fig. 8). The κB-binding activity was strongly reduced in both $p50^{-/-}$ and $relB^{-/-}$ single-mutant mice (8, 21) and almost completely abolished in $p50^{-/-}relB^{-/-}$ double-mutant thymus (Fig. 8 *A*, lanes *1–4*). Challenge with anti-p52 (lanes *5–8*) and anti-RelA (lanes *9–12*) antiserum reduced the respective binding complexes in wild-type or single-mutant mice, and did not reveal any new homodimers or heterodimers in mice lacking p50, RelB, or both. The complex in extracts from p50-deficient single knockouts consisted of p52–RelB heterodimers since it was reduced in $relB^{-/-}$ mice (lanes *3* and *4*) and in the presence of anti-p52 antiserum (lanes *2* and *6*). We were unable to detect significant binding of c-Rel under these conditions, and only the very weak κB-binding activity that remained in extracts from double-knockout mice was reduced by antiserum directed against c-Rel, p52, or RelA (lanes *4*, *8*, *12*, and data not shown). Integrity of extracts was checked with an octamer binding site (lanes *13–16*). Also, no compensatory complexes could be detected in spleen extracts or with κB-binding sites derived from the immunoglobulin κ light chain enhancer or the HIV LTR (data not shown).

In most cells, NF-κB/Rel activities are retained in an inactivated form in the cytoplasm through their interaction with the inhibitory proteins IκBα and IκBβ or the p100 and p105 precursors. These inactive complexes, however, can readily be activated by DOC treatment resulting in increased κB-binding activity (30). Therefore, we analyzed whether any new compensatory complexes can be found in DOC-treated extracts from single- or double-mutant mice (Fig. 8 *B*). Under these conditions, binding of p50 homodimers in wild-type and $relB^{-/-}$ extracts was significantly reduced. In all activated extracts, an additional complex of slower mobility could be observed, although the signal was clearly reduced in the absence of p50, RelB, or both (compare lanes *1–4* and *5–8*). Challenge with anti-

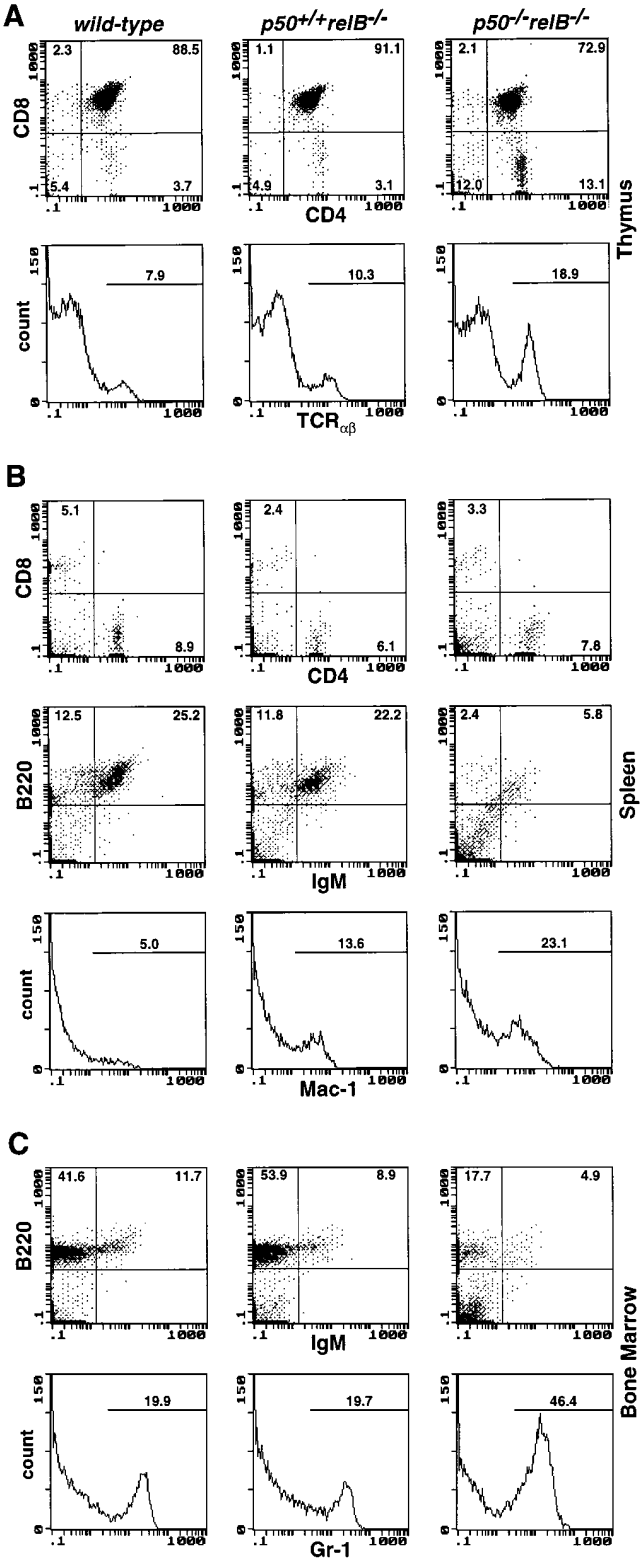

Figure 6. Flow cytometric analysis of 2-wk-old wild-type, $relB^{-/-}$, and $p50^{-/-}relB^{-/-}$ mice. Thymus (*A*), spleen (*B*), and bone marrow (*C*) cell suspensions were analyzed for surface expression of CD4, CD8, TCR-α/β (T cells), B220 and IgM (B cells), Gr-1 (granulocytes), and F4/80 (macrophages). Genotypes are depicted above representative plots. Numbers indicate subpopulation percentages.

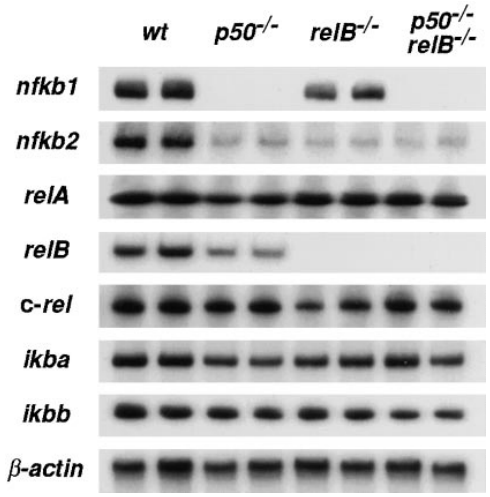

Figure 7. RNA expression analysis in wild-type, $p50^{-/-}$, $relB^{-/-}$, and $p50^{-/-}relB^{-/-}$ mice. Total thymus RNA was prepared from 2-wk-old mice, reverse transcribed, and cDNAs were amplified by semi-quantitative PCR using the indicated specific primers as described in Materials and Methods. Gels were exposed for different times to compensate for differences in the expression levels of individual family members.

RelA and anti–c-Rel antiserum showed that this κB-binding activity most likely consisted of c-Rel homodimers and c-Rel–RelA heterodimers, although RelA homodimers could not be excluded since the anti–c-Rel antiserum weakly cross-reacts against RelA (lanes 9–12 and 13–16 and data not shown). In any case, these complexes were neither increased in single- nor double-mutant mice, indicating the lack of compensatory κB-binding activities in both single- and double-knockout mice.

Discussion

More than 10 potential homodimers and heterodimers can be formed among members of the NF-κB/Rel family of transcription factors that can bind to similar *cis*-regulatory sites and modulate gene expression. This results in a high degree of complexity within this family of transcription factors. Several reports of mice with targeted disruptions of individual NF-κB/Rel family members demonstrated that the different proteins play distinct biological roles (6, 7). It is unclear, however, whether functional redundancy also exists within this family that would result in a (partial) compensation of the phenotype in single-knockout animals.

Severely Increased Pathology in $p50^{-/-}relB^{-/-}$ Double-knockout Mice. Both thymic atrophy and myeloid hyperplasia in bone marrow and spleen were markedly increased in $p50^{-/-}relB^{-/-}$ double-mutant mice compared to $relB^{-/-}$ single-mutant animals. Also, multiorgan inflammation was dramatically increased in severity and extent resulting in premature death of all double-knockout mice. Another notable difference is the penetrance of the pathological changes in thymus and other organs. The phenotype was markedly increased in severity in all $p50^{-/-}relB^{-/-}$ double knockouts examined, whereas there was considerable interanimal vari-

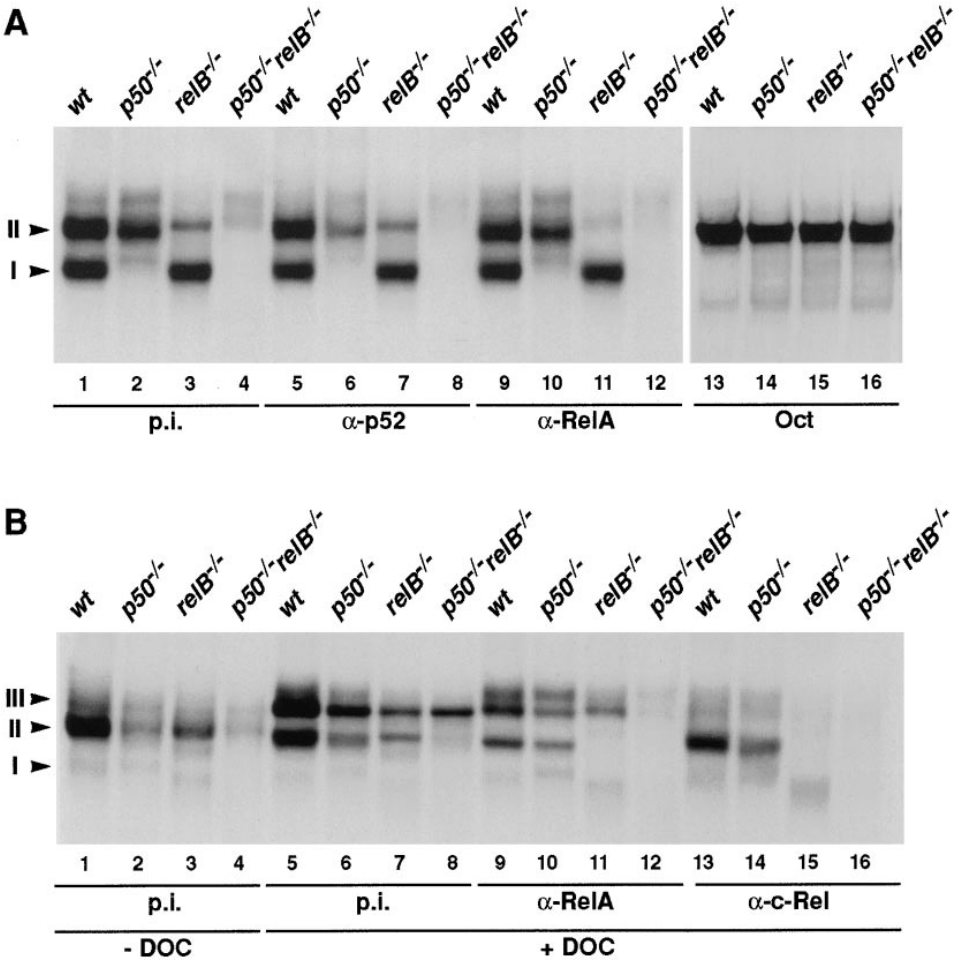

Figure 8. NF-κB/Rel binding activities in wild-type, $p50^{-/-}$, $relB^{-/-}$, and $p50^{-/-}relB^{-/-}$ mice. (*A*) Thymus extracts from 2-wk-old mice were incubated with a palindromic κB-binding site and analyzed by EMSA. Genotypes are shown at the top. The addition of specific antisera against the different members of the NF-κB/Rel family is indicated at the bottom. *p.i.*, Preimmune serum. p50 homodimers (*I*) as well as p50-RelA, p50-RelB, and p52-RelB heterodimers (*II*) are indicated at the left. The same extracts were incubated with an octamer binding site (*Oct*) to demonstrate similar amounts of DNA-binding activity (lanes *13–16*). (*B*) Analysis of NF-κB/Rel complexes in activated extracts. Thymus extracts from wild-type, $p50^{-/-}$, $relB^{-/-}$, and $p50^{-/-}relB^{-/-}$ mice were incubated with a palindromic κB-binding site in the absence (lane *1–4*) or presence (lanes *5–16*) of 0.6% DOC. Genotypes are shown at the top. The addition of specific antisera against the different members of the NF-κB/Rel family is indicated at the bottom. p.i., Preimmune serum. p50 homodimers (*I*) p50-RelA, p50-RelB, and p52-RelB heterodimers (*II*) as well as RelA-c-Rel complexes and c-Rel homodimers (*III*) are indicated at the left.

ation in $relB^{-/-}$ single-knockout mice. Heterozygous $relB^{-/+}$ mice that also lacked p50 had moderate pathological changes that were qualitatively similar to homozygous $relB^{-/-}$ mice, further lending support to the notion that the lack of RelB is partially compensated by other p50-containing complexes.

There are examples to support the theory of functional compensation within a family of related proteins. For instance, embryos that are exposed to retinoic acid during development have a wide spectrum of malformations. Whereas the disruption of individual retinoic acid receptors did not result in the expected phenotypes, double-mutant mice have severe developmental abnormalities (31). Similarly, increased severity in phenotypic changes was observed in mice with combined deficiencies of the homeobox genes *hoxa-3* and *hoxd-3* (32) or the tyrosine kinases Src, Fyn, and Yes (33). Increased expression of a related family member as a compensatory mechanism has been proposed for the myogenic transcription factor Myo D. Mice with a targeted disruption of *myo D* do not have morphological abnormalities in skeletal muscle, but do have markedly increased levels of *myf-5* mRNA. Simultaneous disruption of both *myo D* and *myf-5*, however, results in a more severe phenotype (34). Our results also suggest functional redundancy within the NF-κB/Rel family and, in contrast to Myo-D–deficient mice, we were unable to detect a compensatory upregulation of other NF-κB/Rel family members in both single- and double-knockout animals. Compared to $relB^{-/-}$ single-knockout mice, $p50^{-/-}relB^{-/-}$ double knockouts also lack p50–p50, p50–p52, p50–RelA, and p50–c-Rel complexes. Thus, additional mouse mutants deficient for different combinations of NF-κB/Rel proteins will be necessary to further elucidate the network of redundancy and to understand the specific functions of each NF-κB/Rel family member in more detail.

Role of T Cells in the $relB^{-/-}$ Pathology. Several of the histopathologic features and cellular constituents observed in the lung of $relB^{-/-}$ and $p50^{-/-}relB^{-/-}$ mutant mice are similar to those observed in certain human interstitial lung diseases, including idiopathic pulmonary hemosiderosis (35), Goodpasture's syndrome (36), and acute systemic lupus erythematosis with a hemorrhagic component (37, 38). The inflammatory cell infiltration in $p50^{-/-}relB^{-/-}$ mice, in particular in the skeletal and cardiac musculature, kidney, and salivary glands, resembles that seen in certain human autoimmune diseases, including immune-mediated myocarditis and polymyositis, and Sjögren's syndrome (39, 40). Many experimental models have shown that T cells can be pathogenic mediators in autoimmune diseases (41, 42). Indeed, by using a transgenic mouse line that lacks T cells, we

have recently demonstrated that both multiorgan inflammation and myeloid hyperplasia in RelB-deficient mice are T cell–dependent (43). This result correlates with the finding that the inflammatory infiltrates in 10–20-d-old *relB*$^{-/-}$ single- and *p50*$^{-/-}$*relB*$^{-/-}$ double-knockout mice predominantly consisted of CD4$^+$ and CD8$^+$ T cells. In thymus, RelB expression is restricted to medullary DC and epithelial cells (15, 21, 22), cell types that have been implicated in the process of negative selection (44, 45). Since development of thymic medulla is impaired in the absence of RelB, a defect in clonal deletion of autoreactive T cells may eventually result in potentially pathogenic T cells promoting the inflammatory phenotype observed in RelB-deficient mice. This model is further supported by the finding that *relB*$^{-/-}$ mice poorly delete autoreactive thymocytes and have splenocytes that generate an autoreactive response (46).

The thymus of *p50*$^{-/-}$ mice is nonremarkable and T cell development is not impaired in these animals (8). Despite thymic atrophy and impaired development of a thymic medulla, RelB-deficient mice have normal thymocyte subsets as defined by CD4, CD8, CD3, CD25, and TCR-α/β surface markers (21). Simultaneous disruption of p50 and RelB, however, resulted in a markedly increased thymic atrophy with a 10–20-fold reduction in cellularity, the complete absence of a medullary compartment, and an altered profile of thymocyte subpopulations. Consistent with the thymocyte profile, mature CD4$^+$ and CD8$^+$ single positive cells could be detected in peripheral lymphoid organs and inflammatory infiltrates of double-knockout animals, indicating that T cell differentiation is not blocked in the absence of both p50 and RelB. The basis for the lack of immature CD4$^+$CD8$^+$ DP thymocytes in 3-wk-old *p50*$^{-/-}$ *relB*$^{-/-}$ mice is not clear. Interestingly, very similar changes in thymus have been observed in mice lacking the protooncogene c-*fos* (47). The drastic reduction in the number of CD4$^+$CD8$^+$ DP thymocytes occurs only in 40–50% of the c-*fos*$^{-/-}$ mice, and it has been suggested that this defect could be an indirect consequence of impaired bone marrow function and general stress on these animals (48). Similar mechanisms may be responsible for the dramatic reduction in the number of DP thymocytes in mice lacking both p50 and RelB.

Role of B Cells, Macrophages, and Neutrophils. B cell development in *relB*$^{-/-}$ mice appears normal and B cells lacking RelB undergo normal maturation to Ig secretion and Ig class switching, but they have decreased proliferative responses (21, 49). Immunohistochemical analysis of tissue sections revealed that B cells are a prominent component of the inflammatory infiltrates in *relB*$^{-/-}$ single-mutant animals. Similar to RelB, p50 is not required for normal B cell development (8). However, purified B cells from p50-deficient mice have selective defects in proliferation, differentiation, germ-line C_H transcription, and Ig class switching (9). In contrast to *relB*$^{-/-}$ single mutants, *p50*$^{-/-}$*relB*$^{-/-}$ double-mutant mice did not have significant numbers of B cells in inflamed tissues despite markedly increased severity of the phenotype. This result correlates with impaired B cell development resulting in markedly reduced numbers of both immature B220$^+$IgM$^-$ and mature B220$^+$IgM$^+$ B cells in bone marrow and spleen of double-knockout mice. Thus, B cells appear not to be required for the development of the multiorgan inflammation, although we cannot rule out the possibility that B cells may modulate the inflammatory response in RelB-deficient mice. Further studies, such as in vitro differentiation and bone marrow reconstitution experiments, are required to understand the developmental potential of T and B cells from *p50*$^{-/-}$*relB*$^{-/-}$ mice in more detail.

We also analyzed the contribution of myeloid cells to the inflammatory infiltrate using mAbs specific for macrophages (F4/80) and neutrophils (7/4). In 20-d-old animals, only very few F4/80$^+$ cells were present in the inflammatory infiltrates of both *relB*$^{-/-}$ single- and *p50*$^{-/-}$*relB*$^{-/-}$ double-knockout mice. In 5–6-week-old *relB*$^{-/-}$ single mutants, however, positive F4/80 staining could be detected in the inflammatory infiltrates of liver and lung (data not shown), suggesting that macrophages are not playing a major role during the early stages of the inflammatory phenotype. The faint F4/80 staining of sinusoidal Kupffer cells is most likely due to an activated state of these tissue macrophages triggered by the inflammatory infiltrates, since it has been shown that F4/80 expression is significantly reduced upon antigen stimulation and activation (50). In contrast to macrophages, mature neutrophils contribute to the inflammatory infiltrate in 20-d-old single- and, in particular, double-knockouts. This finding correlates with a marked increased of neutrophils in bone marrow and spleen of *p50*$^{-/-}$*relB*$^{-/-}$ mice compared to *relB*$^{-/-}$ animals. The cause of this prominent neutrophilia is still unclear. One possible explanation is that polymorphonuclear leukocytes become activated by cytokines released by autoreactive T cells, a scenario that is supported by an altered cytokine milieu in mice lacking RelB and an attenuated myeloid hyperplasia in T cell–deficient *relB*$^{-/-}$ mice (21a and 43).

The phenotypic changes in *p50*$^{-/-}$*relB*$^{-/-}$ double-knockout and *p50*$^{-/-}$*relB*$^{-/+}$ mice, compared to the respective single-knockout and *relB*$^{-/+}$ animals, indicate that the lack of RelB is partially compensated by other p50-containing complexes. Our results also show that the classical p50-RelA–NF-κB activity is not required for the development of the multiorgan inflammatory phenotype. Additional NF-κB/Rel double-knockout mice may give further insight into both functional redundancy and specificity within this family.

We gratefully acknowledge Kenneth Class for flow cytometry, Michele French and Sophie Komar for excellent technical assistance, and James Loy for photoimaging. We also thank Violetta Iotsova and Jorge Caa-

mano for valuable comments on this manuscript and all the staff in Veterinary Sciences of Bristol-Myers Squibb.

Address correspondence to Rodrigo Bravo, Department of Oncology, Bristol-Myers Squibb Pharmaceutical Research Institute, PO Box 4000, Princeton, NJ 08543-4000. The present address of W.C. Sha is Department of Molecular and Cell Biology, University of California at Berkeley, Berkeley, CA 94720-3200.

Received for publication 21 January 1997.

References

1. Grilli, M., J.-S. Chiu, and M.J. Lenardo. 1993. NF-κB and Rel-participants in a multiform transcriptional regulatory system. *Int. Rev. Cytol.* 143:1–62.
2. Baeuerle, P.A., and T. Henkel. 1994. Function and activation of NF-κB in the immune system. *Annu. Rev. Immunol.* 12: 141–179.
3. Siebenlist, U., G. Franzoso, and K. Brown. 1994. Structure, regulation and function of NF-κB. *Annu. Rev. Cell Biol.* 10: 405–455.
4. Kopp, E.B., and S. Ghosh. 1995. NF-κB and Rel proteins in innate immunity. *Adv. Immunol.* 58:1–27.
5. Verma, I.M., J.K. Stevenson, E.M. Schwarz, D. Van Antwerp, and S. Miyamoto. 1995. Rel/NF–κB/IκB family: intimate tales of association and dissociation. *Genes Dev.* 9:2723–2735.
6. Baeuerle, P.A., and D. Baltimore. 1996. NF-κB: ten years after. *Cell.* 87:13–20.
7. Baldwin, A.S., Jr. 1996. The NF-κB and IκB proteins, new discoveries and insights. *Annu. Rev. Immunol.* 14:649–681.
8. Sha, W.C., H.-C. Liou, E.I. Tuomanen, and D. Baltimore. 1995. Targeted disruption of the p50 subunit of NF-κB leads to multifocal defects in immune responses. *Cell.* 80:321–330.
9. Snapper, C.M., P. Zelazowski, F.R., Rosas, M.R. Kehry, M. Tian, D. Baltimore, and W.C. Sha. 1996. B cells from p50/NF-κB knockout mice have selective defects in proliferation, differentiation, germ-line C_H transcription, and Ig class switching. *J. Immunol.* 156:183–191.
10. Beg, A.A., W.C. Sha, R.T. Bronson, S. Ghosh, and D. Baltimore. 1995. Embryonic lethality and liver degeneration in mice lacking the RelA component of NF-κB. *Nature (Lond.).* 376:167–169.
11. Köntgen, F., R.J. Grumont, A. Strasser, D. Metcalf, R. Li, D. Tarlinton, and S. Gerondakis. 1995. Mice lacking the *c-rel* proto-oncogene exhibit defects in lymphocyte proliferation, humoral immunity, and interleukin-2 expression. *Genes Dev.* 9:1965–1977.
12. Gerondakis, S., A. Strasser, D. Metcalf, G. Grigoriadis, J.-P.Y. Scheerlinck, and R.J. Grumont. 1996. Rel-deficient T cells exhibit defects in production of interleukin 3 and granulocyte–macrophage colony-stimulating factor. *Proc. Natl. Acad. Sci. USA.* 93:3405–3409.
13. Ryseck, R.-P., P. Bull, M. Takamiya, V. Bours, U. Siebenlist, P. Dobrzanski, and R. Bravo. 1992. RelB, a new Rel family transcription activator that can interact with p50-NF-κB. *Mol. Cell Biol.* 12:674–684.
14. Ryseck, R.-P., F. Weih, D. Carrasco, and R. Bravo. 1996. RelB, a member of the Rel/NF-κB family of transcription factors. *Braz. J. Med. Biol. Res.* 29:895–903.
15. Carrasco, D., R.-P. Ryseck, and R. Bravo. 1993. Expression of *rel*B transcripts during lymphoid organ development: specific expression in dendritic antigen-presenting cells. *Development (Camb.).* 118:1221–1231.
16. Lernbecher T., U. Müller, and T. Wirth. 1993. Distinct NF-κB/Rel transcription factors are responsible for tissue-specific and inducible gene activation. *Nature (Lond.).* 365:767–770.
17. Lernbecher, T., B. Kistler, and T. Wirth. 1994. Two distinct mechanisms contribute to the constitutive activation of RelB in lymphoid cells. *EMBO (Eur. Mol. Biol. Organ.) J.* 13:4060–4069.
18. Weih, F., D. Carasco, and R. Bravo. 1994. Constitutive and inducible Rel/NF-κB activities in mouse thymus and spleen. *Oncogene.* 9:3289–3297.
19. Liou, H.-C., W.C. Sha, M.L. Scott, and D. Baltimore. 1994. Sequential induction of NF-κB/Rel family proteins during B-cell terminal differentiation. *Mol. Cell. Biol.* 14:5349–5359.
20. Granelli-Piperno, A., M. Pope, K. Inaba, and R.M. Steinman. 1995. Coexpression of NF-κB/Rel and Sp1 transcription factors in human immunodeficiency virus 1–induced, dendritic cell–T-cell syncytia. *Proc. Natl. Acad. Sci. USA.* 92; 10944–10948.
21. Weih, F., D. Carrasco, S.K. Durham, D.S. Barton, C.A. Rizzo, R.-P. Ryseck, S.A. Lira, and R. Bravo. 1995. Multiorgan inflammation and hematopoietic abnormalities in mice with a targeted disruption of RelB, a member of the NF-κB/Rel family. *Cell.* 80:331–340.

21a. Weih, F., G. Warr, H. Yang, and R. Bravo. 1997. Multifocal defects in immune responses in RelB-deficient mice. *J. Immunol.* In press.

22. Burkly, L., C. Hession, L. Ogata, C. Reilly, L.A. Marconi, D. Olson, R. Tizard, R. Cate, and D. Lo. 1995. Expression of *rel*B is required for the development of thymic medulla and dendritic cells. *Nature (Lond.).* 373:531–536.
23. Kunsch, C., S.M. Ruben, and C.A. Rosen. 1992. Selection of optimal κB/Rel DNA-binding motifs: interaction of both subunits of NF-κB with DNA is required for transcriptional activation. *Mol. Cell. Biol.* 12:4412–4421.
24. Dobrzanski, P., R.-P. Ryseck, and R. Bravo. 1993. Both N- and C-terminal domains of RelB are required for full transactivation: role of the N-terminal leucine zipper-like motif. *Mol. Cell. Biol.* 13:1572–1582.
25. Lin, R., D. Gewert, and J. Hiscott. 1995. Differential transcriptional activation *in vitro* by NF-κB/Rel proteins. *J. Biol. Chem.* 270:3123–3131.
26. Laird, P.W., A. Zijderveld, K. Linders, M.A. Rudnicki, R. Jaenisch, and A. Berns. 1991. Simplified mammalian DNA isolation procedure. *Nucleic Acids Res.* 19:4293–4296.
27. Coligan, J.E., A.M. Kruisbeek, D.H. Margulies, E.M. Shevach, and W. Strober. 1992. Isolation and fractionation of mononuclear cell populations. *In* Current Protocols in Immunology. J.W. & Sons, editor. Greene Publishing Associates & Wiley-Interscience, New York. 3.1.1–3.1.5.
28. Mumberg, D., F.C. Lucibello, M. Schuermann, and R. Müller. 1991. Alternative splicing of *fos*B transcripts results in differentially expressed mRNAs encoding functionally antagonistic proteins. *Genes Dev.* 5:1212–1223.

29. Carrasco, D., C.A. Rizzo, K. Dorfman, and R. Bravo. 1996. The v-*rel* oncogene promotes malignant T-cell leukemia/lymphoma in transgenic mice. *EMBO (Eur. Mol. Biol. Organ.) J.* 15:3640–3650.
30. Baeuerle, P.A. 1991. The inducible transcription activator NF-κB: regulation by distinct protein subunits. *Biochim. Biophys. Acta.* 1072:63–80.
31. Chambon, P. 1994. The retinoid signaling pathway: molecular and genetic analyses. *Semin. Cell Biol.* 5:115–125.
32. Condie, B.G., and M.R. Capecchi. 1994. Mice with targeted disruptions in the paralogous genes hoxa-3 and hoxd-3 reveal synergistic interactions. *Nature (Lond.).* 370:304–307.
33. Stein, P.L., H. Vogel, and P. Soriano. 1994. Combined deficiencies of Src, Fyn, and Yes tyrosine kinases in mutant mice. *Genes Dev.* 8:1999–2007.
34. Rudnicki, M.A., P.N. Schnegelsberg, R.H. Stead, T. Braun, H.H. Arnold, and R. Jaenisch. 1993. MyoD or Myf-5 is required for the formation of skeletal muscle. *Cell.* 75:1351–1359.
35. Soergel, K.H., and S.C. Sommer. 1962. Idiopathic pulmonary hemosiderosis and related syndromes. *Am. J. Med.* 32: 499–511.
36. Donald, K.J., R.L. Edwards, and J.D.S. McEvot. 1975. Alveolar capillary basement membrane lesions in Goodpasture's syndrome and idiopathic pulmonary hemosiderosis. *Am. J. Med.* 59:642–649.
37. Matthay, R.A., M.I. Schwarz, T.L. Petty, R.E. Stanford, R.C. Gupta, S.A. Sahn, and J.C. Steigerwald. 1975. Pulmonary manifestations of systemic lupus erythematosis. Review of twelve cases of acute lupus pneumonitis. *Medicine (Baltimore).* 54:397–409.
38. Hunninghake, G.W., and A.S. Fauci. 1979. Pulmonary involvement in the collagen vascular diseases. *Am. Rev. Respir. Dis.* 119:471–503.
39. Cronin, M.E., F.W. Miller, and P.H. Plotz. 1988. Polymyositis and dermatomyositis. *In* Primer on the Rheumatic Diseases. J.H.R. Schumacher, editor. Arthritis Foundation, Atlanta. 120–123.
40. Talal, N. 1988. Sjögren's syndrome. *In* Primer on the Rheumatic Diseases. J.H.R. Schumacher, editor. Arthritis Foundation, Atlanta. 136–138.
41. Kumar, V., D.H. Kono, J.L. Urban, and L. Hood. 1989. The T-cell receptor repertoire and autoimmune disease. *Annu. Rev. Immunol.* 7:657–682.
42. Theofilopoulos, A.N. 1995. The basis of autoimmunity: part I mechanisms of aberrant self-recognition. *Immunol. Today.* 16:90–123.
43. Weih, F., S.K. Durham, D.S. Barton, W.C. Sha, D. Baltimore, and R. Bravo. 1996. Both multiorgan inflammation and myeloid hyperplasia in RelB-deficient mice are T cell dependent. *J. Immunol.* 157:3974–3979.
44. Nossal, G.J.V. 1994. Negative selection of lymphocytes. *Cell.* 76:229–239.
45. Robey, E., and B.J. Fowlkes. 1994. Selective events in T cell development. *Annu. Rev. Immunol.* 12:675–705.
46. Laufer, T.M., J. DeKoning, J.S. Markowitz, D. Lo, and L.H. Glimcher. 1996. Unopposed positive selection and autoreactivity in mice expressing class II MHC only in thymic cortex. *Nature (Lond.).* 383:81–90.
47. Wang, Z-Q., C. Ovitt, A.E. Grigoriadis, U. Möhle-Steinlein, U. Rüther, and E.F. Wagner. 1992. Bone and haematopoietic defects in mice lacking c-*fos*. *Nature (Lond.).* 360: 741–745.
48. Okada, S., Z.-Q. Wang, A.E. Grigoriadis, E.F. Wagner, and T. von Rüden. 1994. Mice lacking c-*fos* have normal hematopoietic stem cells but exhibit altered B-cell differentiation due to an impaired bone marrow environment. *Mol. Cell. Biol.* 14:382–390.
49. Snapper, C.M., F.R. Rosas, P. Zelazowski, M.A. Moorman, M.R. Kehry, R. Bravo, and F. Weih. 1996. B cells lacking RelB are defective in proliferative responses, but undergo normal B cell maturation to Ig secretion and Ig class switching. *J. Exp. Med.* 184:1537–1541.
50. Austyn, J.M., and S. Gordon. 1981. F4/80, a monoclonal antibody directed specifically against the mouse macrophage. *Eur. J. Immunol.* 11:805–815.